

# 1 Do phenomenological dynamical paleoclimate models have physical similarity 2 with “Nature”? Seemingly, not all of them do.

3 Mikhail Y. Verbitsky<sup>1,2</sup> and Michel Crucifix<sup>2</sup>

4 <sup>1</sup>Gen5 Group, LLC, Newton, MA, USA

5 <sup>2</sup>UCLouvain, Earth and Life Institute, Louvain-la-Neuve, Belgium

6  
7 Correspondence: Mikhaïl Verbitsky (verbitskys@gmail.com)

8  
9 **Abstract.** Phenomenological models may be impressive in reproducing empirical time series but this  
10 is not sufficient to claim physical similarity with Nature until comparison of similarity parameters is  
11 performed. We illustrated such a process of diagnostics of physical similarity by comparing the  
12 phenomenological dynamical paleoclimate model of Ganopolski (2023), the van der Pol model (as used  
13 by Crucifix, 2013), and the model of Leloup and Paillard (2022) with the physically explicit Verbitsky *et*  
14 *al* (2018) model that played a role of a reference dynamical system. We concluded that phenomenological  
15 models of Ganopolski (2023) and of Leloup and Paillard (2022) may be considered to be physically  
16 similar to the proxy parent dynamical system in some range of parameters, or in other words they may be  
17 derived from basic laws of physics under some reasonable physical assumptions. We have not been able  
18 to arrive to the same conclusion regarding the van der Pol model. Though developments of better proxies  
19 of the parent dynamical system should be encouraged, we nevertheless believe that the diagnostics of  
20 physical similarity, as we describe it here, should become a standard procedure to delineate a model that  
21 is merely a statistical description of the data, from a model that can be claimed to have a link with known  
22 physical assumptions.

23 The similarity parameters we advance here as the key dimensionless quantities are the ratio of the  
24 astronomical forcing amplitude to the terrestrial ice-sheet mass influx and the so-called *V*-number that is  
25 the ratio of the amplitudes of time-dependent positive and negative feedbacks. We propose to use  
26 available physical models to discover additional similarity parameters that may play central roles in ice-  
27 age rhythmicity. Finding values for these similarity parameters should become a central objective of  
28 future research into glacial-interglacial dynamics.

## 29 30 31 1. Introduction.

32 A mathematical model that is constructed to understand a physical phenomenon must be simple  
33 enough, otherwise the interpretation of the modeling results may be as difficult as the interpretation of  
34 direct observations. In that regard, even most sophisticated space-resolving models of global climate  
35 provide, indeed, a simplified picture of the phenomenon, but a much more drastic degree of simplification  
36 is required when we study climate on timescales of tens of thousands of years. Faced with this challenge,  
37 Barry Saltzman used to be a proponent of the phenomenological approach “through the construction of  
38 low-order models in which the full behavior is projected onto the dynamics of a reduced number of  
39 ...highly aggregated variables...” (Saltzman, 2002). Phenomenological models of paleoclimate variability  
40 have routinely been used to explain certain characteristics of glacial-interglacial cycles (e.g., Saltzman  
41 and Maasch, 1991, Saltzman and Verbitsky, 1992, 1993, 1994, Paillard, 1998, Tziperman et al, 2006,  
42 Crucifix, 2013, Kaufmann and Pretis, 2021, Talento and Ganopolski, 2021, Leloup and Paillard, 2022,  
43 Ganopolski, 2023). The core principle of the phenomenological approach is to fit model-produced time  
44 series to the observational time series. When this goal is achieved, it is tacitly assumed that there must be  
45 some physical similarity between the phenomenological model and Nature. We believe though that the  
46 assumption of physical similarity with Nature can be more rigorously challenged before the implications  
47 of a phenomenological model are accepted.

48 In fluid dynamics, for example, the concept of physical similarity is the cornerstone of any judgement  
49 built on model experimentations. Classical similarity parameters, which emerge from the analysis of

50 fundamental conservation laws, like the Reynolds number, the Peclet number, the Euler number, etc.,  
 51 quantify the relative importance of different aspects of fluid flow. For an experimental or a numerical  
 52 model to be relevant, it should have quantitatively the same similarity parameters as those of the natural  
 53 phenomenon being considered. We will now apply this concept of physical similarity to dynamical  
 54 paleoclimate systems.

55 As physicists, we might want to describe a phenomenon such as ice ages as “emerging from  
 56 fundamental laws”. However, the fundamental laws that we know in physics dictate interactions between  
 57 particles. Perhaps one of the greatest challenges of the physical approach to complex systems is to explain  
 58 how Nature organizes billions of billions of particles in interaction to generate some predictable behavior  
 59 even on very long time scales such as, precisely, glacial-interglacial cycles. The methods of statistical  
 60 physics tell us how to define macroscopic variables to describe the collective behavior of particles  
 61 submitted to a conservation constraint, and how the phenomenon of dissipation emerges as a consequence  
 62 of statistical mixing in a chaotic system. Dynamical system’s theory tells us why we mainly see the most  
 63 unstable modes of a system (Haken, 2006) and how time scale separation assumptions allow us to focus  
 64 on a subset of the system’s variables. In a nutshell, the theories of mathematical and statistical physics  
 65 make it legitimate to assume that there is a natural parent dynamical system with much fewer degrees of  
 66 freedom than Avogadro’s number, and which has generated the phenomenon that we see.

67 What “much fewer” means is not a straightforward matter. It depends on what we describe as the  
 68 phenomenon, and how fine-grained this description is. For example, the successions of glacial-interglacial  
 69 cycles and the timing of deglaciations appear to follow fairly simple, predictable rules (Tzedakis et al.,  
 70 2017). Hence, it is legitimate to assume that the physical parent dynamical system, which dictates the  
 71 evolution of the macroscopic state of climate at the orbital time scale, can be reduced to a small number  
 72 of degrees of freedom.

73 Specifically, we may suggest that this parent dynamical system is governed by  $n$  physical parameters  
 74  $a_i$  such that a dependent variable of interest,  $x$ , can be expressed as function

$$75 \quad 76 \quad x = \varphi(a_1, a_2, \dots, a_i, \dots, a_n) \quad (1)$$

77 If  $k$  parameters of  $a_1, a_2, \dots, a_i, \dots, a_n$  are parameters with independent dimensions, then, according to  $\pi$ -  
 78 theorem (Buckingham, 1914), in the dimensionless form, the phenomenon (1) can be described by  
 79  $m = n - k$  adimensional similarity parameters  $\Pi_1, \Pi_2, \dots, \Pi_i, \dots, \Pi_m$ :

$$80 \quad \Pi = \Phi(\Pi_1, \Pi_2, \dots, \Pi_i, \dots, \Pi_m) \quad (2)$$

81 Two physical phenomena have physical similarity if both of them are described in the adimensional  
 82 form by the same function  $\Phi(\Pi_1, \Pi_2, \dots, \Pi_i, \dots, \Pi_m)$  and have identical numerical values of similarity  
 83 parameters  $\Pi_1, \Pi_2, \dots, \Pi_i, \dots, \Pi_m$ , though numerical values of the governing parameters  
 84  $a_1, a_2, \dots, a_i, \dots, a_n$  may be different (e.g., Barenblatt, 2003).

85 As we have already mentioned, our knowledge about a parent dynamical system is suggested to us by  
 86 the presence of empirical time series. It means that one of the similarity parameters, say  $\Pi_1$ , is  
 87 adimensional time  $\frac{t}{\tau}$  ( $t$  and  $\tau$  are dimensional time and a timescale, correspondingly), and all other  
 88 parameters  $\Pi_2, \dots, \Pi_i, \dots, \Pi_m$  are fixed to specific values. Hence, an experimental time series (neglecting  
 89 measure errors) can be described as

$$90 \quad 91 \quad \Pi = \Phi\left(\frac{t}{\tau}, \Pi_2, \dots, \Pi_i, \dots, \Pi_m\right) \quad (3)$$

92 If we created a model dynamical system such that it is governed by  $p$  governing parameters  $b_i$

$$93 \quad x = \psi(b_1, b_2, \dots, b_i, \dots, b_p) \quad (4)$$

94 and  $r$  parameters of  $b_1, b_2, \dots, b_i, \dots, b_p$  are parameters with independent dimensions, then, again,  
 95 according to  $\pi$ -theorem, in the dimensionless form, the model can be described by  $q = p - r$   
 96 adimensional similarity parameters  $\pi_1, \pi_2, \dots, \pi_i, \dots, \pi_q$ :

$$97 \quad \pi = \Psi(\pi_1, \pi_2, \dots, \pi_i, \dots, \pi_q) \quad (5)$$

98 For a specific time series, and for a fixed set of parameters  $\pi_2, \dots, \pi_i, \dots, \pi_q$ , the model (5) can be  
 99 presented as

$$100 \quad \pi = \Psi\left(\frac{t}{\tau}, \pi_2, \dots, \pi_i, \dots, \pi_q\right) \quad (6)$$

101 The essence of the phenomenological approach is to fit the function  $\Psi\left(\frac{t}{\tau}, \pi_2, \dots, \pi_i, \dots, \pi_q\right)$  to the  
 102 function  $\Phi\left(\frac{t}{\tau}, \Pi_2, \dots, \Pi_i, \dots, \Pi_m\right)$  under the “best” set of parameters  $\pi_2, \dots, \pi_i, \dots, \pi_q$ , i.e. to equate the  
 103 model time series  $\Psi\left(\frac{t}{\tau}, \pi_2, \dots, \pi_i, \dots, \pi_q\right)$  and the natural, empirical, time series  $\Phi\left(\frac{t}{\tau}, \Pi_2, \dots, \Pi_i, \dots, \Pi_m\right)$ :

$$104 \quad \Psi\left(\frac{t}{\tau}, \pi_2, \dots, \pi_i, \dots, \pi_q\right) = \Phi\left(\frac{t}{\tau}, \Pi_2, \dots, \Pi_i, \dots, \Pi_m\right) \quad (7)$$

105 It is obvious that even if the goal (7) is achieved at every  $\frac{t}{\tau}$ -point, we still cannot claim the model (6)  
 106 to be physically similar to “Nature” (3) until we prove that  $\pi_i = \Pi_i$ , i.e.,  $\pi_i$ -physics in the model is as  
 107 significant as the  $\Pi_i$ -physics of Nature. Simply speaking, merely *matching a proposed phenomenological*  
 108 *model with empirical data does not make a case for physical similarity* because it does not provide an  
 109 evidence that it happens for the right reason, the reason being the similarity parameters of the right value,  
 110 i.e.,  $\pi_i = \Pi_i$ .

111 But how can we compare  $\pi_i$ -physics of the phenomenological model and  $\Pi_i$ -physics of Nature if the  
 112 phenomenological models are not derived from the laws of physics? Though, indeed, phenomenological  
 113 models have not been derived from the laws of physics, they are not completely ignorant of the physical  
 114 content: they still have a physical, measurable variable, time; they also have orbital and terrestrial  
 115 forcings as well as positive and negative feedbacks. If the parent dynamical system was formulated in  
 116 terms of similarity parameters formed by the ratios of timescales and by the ratios of the forcings’ and  
 117 feedbacks’ amplitudes, then the comparison with phenomenological models that also use time scales and  
 118 forcing and feedback ratios would be possible. The VCV18 model (Verbitsky et al, 2018), is one such  
 119 candidate (a proxy) for a parent dynamical system. VCV18 was *derived* from the scaled mass- and heat-  
 120 balance equations of the non-Newtonian ice flow. Next, we will derive scaling laws and similarity  
 121 parameters for three phenomenological models: (a) the model of Ganopolski (2023); (b) van der Pol  
 122 model as it has been described by Crucifix (2013); and (c) the model of Leloup and Paillard (2022);  
 123 G23, VDP and LP22, thereafter, respectively. Each of these models produces a specific  
 124 function  $\Psi(\pi_1, \pi_2, \dots, \pi_i, \dots, \pi_q)$ . We then compare functions  $\Psi(\pi_1, \pi_2, \dots, \pi_i, \dots, \pi_q)$  of these models  
 125 with the corresponding function  $\Phi(\Pi_1, \Pi_2, \dots, \Pi_i, \dots, \Pi_m)$  provided by VCV18 to recognize or reject the  
 126 hypothesis of physical similarity with a proxy for the parent dynamical system.

127 Certainly, we cannot expect that the time series produced by G23, VDP, and LP22 models and by the  
 128 VCV18 model are identical, and therefore these models will not be physically similar in the most rigorous  
 129 sense of the equation (7). We will demonstrate though that the answer to the physical-similarity question  
 130 is insightful if our dependent variable of interest  $x$  is not necessarily a time series but a time-independent  
 131 attribute such as the period of glacial rhythmicity. All models of this study reproduce equally well  $\sim 100$ -  
 132 kyr period of the late Pleistocene glaciations. We will now evaluate if the similarity parameters involved  
 133 in the corresponding equations (7) are quantitatively the same.

134  
 135

136 **2. Method**

137  
138 **2.1 VCV18 model as a proxy for a parent dynamical system.**

139  
140 Deriving a low-order dynamical paleoclimate model that may be considered as a candidate (a proxy)  
141 parent dynamical system is not a trivial exercise. The “low-order” challenge means that out of the  
142 multitude of physical phenomena involved only few should be recognized as dominant ones, and the  
143 “dynamical” challenge means that the space-resolving properties should be sensibly reduced to some  
144 integrated variables. Accordingly, in developing VCV18 proxy parent dynamical system, we first  
145 assumed that ice ages can be explained by only two components of the global climate system, continental  
146 ice sheets and the ocean representing the rest of the climate. For an ice sheet we adopted mass,  
147 momentum, and heat conservation equations of a “thin” layer of homogeneous non-Newtonian ice, and  
148 the rest of the climate was represented by the energy-balance equation. To migrate from the three-  
149 dimensional to dynamical equations we used scaling analysis that provides simple mathematical  
150 statements that are consistent with the original physics. Accordingly, the VCV18 dynamical model of the  
151 ice-climate system is defined by the following set of equations:

152 
$$\frac{dS}{dt} = \frac{4}{5} \zeta^{-1} S^{3/4} (\hat{a} - \varepsilon F - \kappa \omega - c\theta) \quad (8)$$

153 
$$\frac{d\theta}{dt} = \zeta^{-1} S^{-1/4} (\hat{a} - \varepsilon F - \kappa \omega) \{ \alpha \omega + \beta [S - S_0] - \theta \} \quad (9)$$

154 
$$\frac{d\omega}{dt} = -\gamma [S - S_0] - \frac{\omega}{\tau} \quad (10)$$

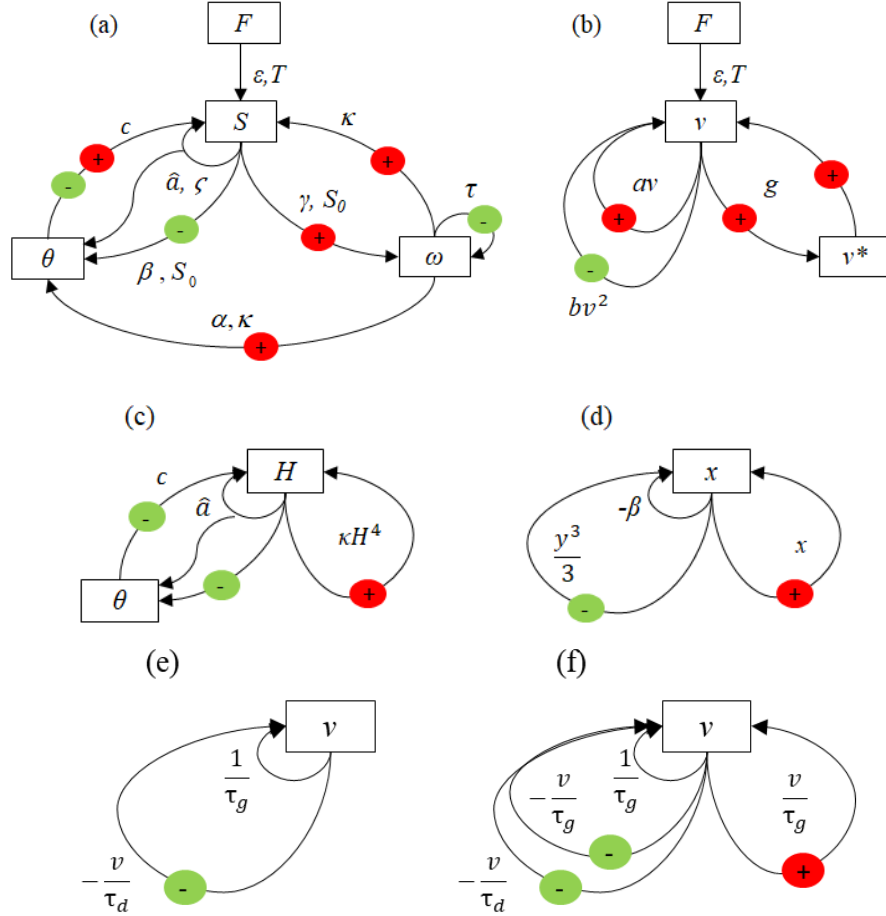
155  
156 Here,  $S$  ( $\text{m}^2$ ) is the area of glaciation,  $\theta$  ( $^{\circ}\text{C}$ ) is the basal ice-sheet temperature, and  $\omega$  ( $^{\circ}\text{C}$ ) is the global  
157 temperature of the rest of the climate. Equation (8) represents global ice balance  $\frac{d(HS)}{dt} = AS$ , where the  
158 ice thickness  $H$  is determined from the thin-layer approximation of ice flow,  $H = \zeta S^{1/4}$ ,  $\zeta$  is dimensional  
159 profile factor (Verbitsky and Chalikov, 1986) and  $A = \hat{a} - \varepsilon F - \kappa \omega - c\theta$  is the surface mass influx.  
160 Equation (9) describes vertical ice temperature advection with a time scale  $H/(\hat{a} - \varepsilon F - \kappa \omega)$ , and  
161 equation (10) is the global energy-balance equation. The parameter  $\hat{a}$  ( $\text{m s}^{-1}$ ) is the snow precipitation  
162 rate;  $F$  is normalized external forcing, i.e., mid-July insolation at  $65^{\circ}\text{N}$  (Berger and Loutre, 1991) of the  
163 amplitude  $\varepsilon$  ( $\text{m s}^{-1}$ );  $\kappa \omega$  represents fast positive feedback from the global climate on ice-sheet mass  
164 balance;  $c\theta$  is the ice discharge due to ice-sheet basal sliding incorporating (both delayed due to the  
165 vertical temperature advection) positive feedback from the global temperature,  $\alpha \omega$ , and a negative  
166 feedback of basal temperature reaction to the changes of ice geometry  $\beta [S - S_0]$ . Further,  $-\gamma [S - S_0]$  is  
167 external forcing for global temperature (e.g., albedo);  $\kappa$  ( $\text{m s}^{-1} \text{ } ^{\circ}\text{C}^{-1}$ ),  $c$  ( $\text{m s}^{-1} \text{ } ^{\circ}\text{C}^{-1}$ ),  $\alpha$  (adimensional),  $\beta$   
168 ( $^{\circ}\text{C m}^{-2}$ ) and  $\gamma$  ( $^{\circ}\text{C m}^{-2} \text{ s}^{-1}$ ) are sensitivity coefficients;  $S_0$  ( $\text{m}^2$ ) is a reference glaciation area; and  $\tau$  (s) is the  
169 global-temperature timescale.

170 Schematically, the dynamical system (8) – (9) is shown in Fig. 1(a). It can be seen that the dynamics  
171 of the VCV18 system is defined by the amplitude and periodicity of the orbital forcing,  $\varepsilon, T$ , by the  
172 terrestrial forcing  $\hat{a}$ , and by three feedback loops: the fast positive feedback,  $-\kappa \omega$ , and by two delayed,  
173 positive and negative feedbacks, combined in the term  $-c\theta$ . The dimensional analysis of the VCV18  
174 model has been performed previously (Verbitsky and Crucifix, 2020, 2021, Verbitsky, 2022a). It was  
175 revealed that its large-scale periodicity is generally governed by two dimensionless parameters: the ratio  
176 of the astronomical forcing amplitude  $\varepsilon$  to the terrestrial ice-sheet mass influx,  $\Pi_2 = \varepsilon/\hat{a}$  and the so-called  
177  $V$ -number,  $\Pi_3 = V$  that is the ratio of amplitudes of time-dependent positive and negative feedbacks.  
178 Specifically, the period  $P$  of the VCV18 system response to the astronomical forcing of period  $T$  is of the  
179 form (hereafter called the “ $P$ -scaling law”):

180  $\frac{P}{T} = \Phi\left(\frac{\varepsilon}{\hat{a}}, V\right)$  (11)

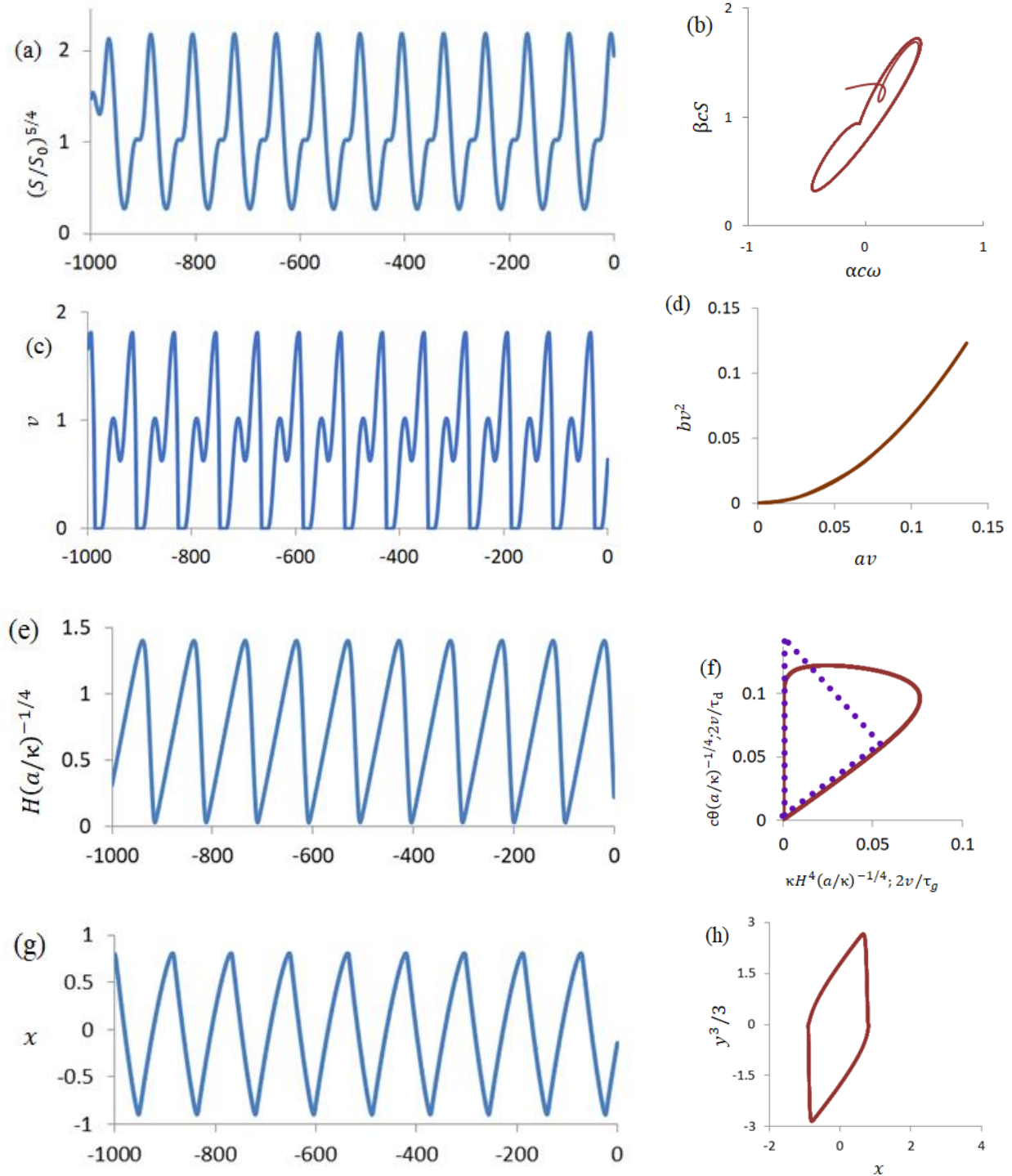
181 For  $T = 40$  kyr,  $\frac{\varepsilon}{\hat{a}} = 1.4$ ,  $V = 0.7$ ,  $\Phi = 2$  (obliquity-period doubling). The corresponding time series and  
 182 positive-versus-negative feedback evolution are shown in Fig. 2 (a, b).

183



184

185 **Figure 1.** (a) The parent dynamical system VCV18 (Eqs. 8–10). Red circles mark positive feedback loops  
 186 and green circles mark negative feedback loops; (b) The same for the G23 phenomenological model (Eqs.  
 187 12-13); (c) The same for simplified system VCV18-1 (Eqs. 22–23); (d) The same for VDP model (Eqs.  
 188 30-31); (e) The same for LP22 model (Eqs. 37-38),  $I = 0$ ; (f) The same for LP22 model (Eqs. 44-45);



190  
 191 **Figure 2.** Time series (kyr BP) and corresponding positive-vs-negative feedback loops: (a, b) VCV18  
 192 (Eqs. 8–10),  $(\frac{S}{S_0})^{5/4}$  is normalized ice volume; (c, d) G23 (Eqs. 12-13); (e, f) VCV18-1 (Eqs. 22–23); all  
 193 variables are normalized by characteristic ice thickness,  $H' = (\hat{a}/\kappa)^{1/4}$ ; the dotted triangle corresponds to  
 194 LP22 (Eqs. 37-38) without astronomical forcing; (g, h) VDP (Eqs. 30-31).  
 195

196 2.2 G23 model.

197 The G23 model (specifically, Model 2, as it is annotated in Ganopolski, 2023) describes evolution of  
 198 global ice volume  $v$  (adimensional) as a response to orbital forcing  $\varepsilon F$  ( $F$  is normalized external forcing  
 199 of the amplitude  $\varepsilon$ ):

$$200 \frac{dv}{dt} = \frac{av - bv^2 - \varepsilon F + d}{1 - \delta g v^*} \quad (12)$$

$$201 \quad 202 v^* = \frac{1}{T^*} \int_{t-T^*}^t v(t') dt' \quad (13)$$

204 The term  $\delta g v^*$  represents an additional positive feedback activated ( $\delta = \delta_1 = 1$ ) when  $\frac{dv}{dt} < 0$ .  
 205 When  $\frac{dv}{dt} \geq 0$ ,  $\delta = \delta_2 = 0$ . Graphically, the dynamical system (12) – (13) is shown in Fig. 1(b). We  
 206 observe that the dynamics of the G23 system is, like VCV18, defined by the amplitude and periodicity of  
 207 the orbital forcing,  $\varepsilon, T$  and by three feedback loops: two positive feedbacks,  $av, gv^*$  and by one negative  
 208 feedback,  $-bv^2$ . Unlike VCV18, though, all feedbacks are instantaneous. We now review how these  
 209 differences may be reflected in the corresponding  $P$ -scaling law.

210 For the purpose of dimensional analysis, we consider Eqs. (12) – (13) in dimensional form assuming  
 211 the following dimensions for variables and parameters involved:  $t$  (s),  $v$  ( $\text{m}^3$ ),  $a$  ( $\text{s}^{-1}$ ),  $b$  ( $\text{m}^{-3}\text{s}^{-1}$ ),  $\varepsilon$  ( $\text{m}^3\text{s}^{-1}$ ),  $F$   
 212 is an adimensional function of the period  $T$  (s),  $d$  ( $\text{m}^3\text{s}^{-1}$ ),  $\delta_1, \delta_2$  (adimensional),  $g$  ( $\text{m}^{-3}$ ),  $v^*$  ( $\text{m}^3$ ). The  
 213 period of the system response to the astronomical forcing is then a function of the following governing  
 214 parameters:

$$215 \quad 216 P = \psi(a, b, \varepsilon, T, d, \delta_1, \delta_2, g) \quad (14)$$

217  
 218 For more explicit physical interpretation, instead of the parameter  $b$ , we will use parameter  $\hat{a} = \frac{a^2}{b}$ ,  
 219 ( $\text{m}^3\text{s}^{-1}$ ), which is the mean growth rate. Also, for the reference values of parameters, provided by  
 220 G23,  $d \ll \varepsilon$ , and, lastly,  $\delta_1, \delta_2$  are constant. Therefore we can re-write (14) as:

$$221 \quad 222 P = \psi(a, \hat{a}, \varepsilon, T, g) \quad (15)$$

223  
 224 If we choose  $\hat{a}, T$  as parameters with independent dimensions, then according to  $\pi$ -theorem:

$$225 \quad 226 \frac{P}{T} = \Psi\left(\frac{\varepsilon}{\hat{a}}, T a, T g \hat{a}\right) \quad (16)$$

227  
 228 Let us now determine the  $V$ -number for G23 as the ratio of amplitudes of time-dependent positive and  
 229 negative feedbacks. Obviously, such ratio should be completely defined by the internal (terrestrial) G23  
 230 properties and therefore:

$$231 \quad 232 V = \lambda(a, b, g) \quad (17)$$

233  
 234 If we choose  $a$  and  $b$  as parameters with independent dimensions, then according to  $\pi$ -theorem:

$$235 \quad 236 V = \Lambda\left(\frac{ga}{b}\right) \quad (18)$$

237  
 238 We can also express  $g$  as a function of  $V$ :

$$239 \quad 240 \frac{ga}{b} = \Lambda^{-1}(V) \quad (19)$$



241  
242 Accordingly, the  $P$ -scaling law of G23 can be written as:  
243

$$244 \frac{P}{T} = \Psi \left[ \frac{\varepsilon}{\hat{a}}, T\alpha, T\alpha\Lambda^{-1}(V) \right] \quad (20)$$

245  
246 or

$$247 \frac{P}{T} = \Psi \left( \frac{\varepsilon}{\hat{a}}, \frac{T}{\tau}, V \right); \tau = 1/\alpha \quad (21)$$

249 We see that the scaling law (21) is different from the scaling law (11) because the  $\Psi$  – function of (21)  
250 depends on  $T$  unlike the  $\Phi$  – function of (11). There are only two scenarios for orbital periods to escape  
251 the  $\Psi$  – function (or the  $\Phi$  – function) in a scaling law. First, they may be excluded from the governing  
252 equations when the main period of system’s variability is attributed to the internal, terrestrial, physics.  
253 This is the case for VDP and LP22 models that will be considered later, but, definitely, it is not applicable  
254 neither to G23 nor VCV18. The second scenario occurs when a system incorporates multiple parameters  
255 encoding different time scales. The interplay of these parameters may create a situation when  $T$ -  
256 dependent similarity parameters form jointly a  $T$ -independent conglomerate similarity parameter, giving a  
257 system the so-called property of incomplete similarity (Barenblatt, 2003). This property has been  
258 discovered for VCV18 (Verbitsky, 2022a). As the result, the  $\Phi$  – function of the scaling law (11) does  
259 not depend on orbital period ( $\Phi = 2$  in the range of  $T = 35 - 60$  kyr). Contrarily, as we have already  
260 noted, G23 positive and negative feedbacks are instantaneous, G23 single ice-growth timescale  $\tau \sim 1/\alpha$   
261 does not have a “counterpart” for an interplay, and therefore the  $\Psi$  – function of (21) is period- $T$   
262 dependent.

263 Nevertheless, for  $T = 40$  kyr,  $\frac{\varepsilon}{\hat{a}} = 1.6$ ,  $V = 1.1$ ,  $\Psi = 2$  (obliquity-period doubling). Hence, *only for*  
264 *the obliquity forcing*, VCV18 and G23 models appear to be physically similar in regards of two,  
265 **quantitatively close** similarity parameters,  $\frac{\varepsilon}{\hat{a}}$ , the ratio of the astronomical forcing amplitude  $\varepsilon$  to the  
266 growth rate  $\hat{a}$ , and in terms of the  $V$ -number. The corresponding time series and positive-versus-negative  
267 feedback evolution are shown in Fig. 2 (c, d). **Geometrically, the similarity between VCV18 and G23**  
268 **models in terms of the  $V$ -number emerges from Fig. 2 (b) and Fig. 2 (d) as similar slopes of the**  
269 **corresponding feedback loops, though, indeed, the instantaneous nature of G23 feedbacks makes their**  
270 **“loop” asymptotically thin.**

271

### 272 **2.3 Simplified VCV18 model (VCV18-1) as a proxy for a parent dynamical system**

273

274 The next phase of our study is devoted to two phenomenological models, VDP and LP22 that have  
275 100-kyr auto-oscillations independently of orbital forcing. To make the diagnostics of physical similarity  
276 possible, we have to further simplify VCV18 system with several, physically reasonable, assumptions:

- 277 (a) Since the global-temperature timescale in equation (10) is much faster than other timescales  
278 (orbital, ice accumulation, and ice-temperature advection), we assume that global temperature is  
279 an instantaneous function of the glaciation forcing,
- 280 (b) In equation (9), we assume  $\alpha = 0$  (for example, effect of increased global temperature is offset  
281 by increased snow precipitation rate, see experiment D in the Appendix of VCV18), which  
282 cancels the direct effect of climate on basal temperature,
- 283 (c) We rewrite equations (8) and (9) in terms of ice thickness  $H = \zeta S^{1/4}$ , and finally
- 284 (d) We attribute all system variability to terrestrial causes ( $\varepsilon = 0$ ).

285 The simplified dynamical system then takes the following form:



286  $\frac{dH}{dt} = \hat{a} + \kappa H^4 - c\theta$  (22)

287

288  $\frac{d\theta}{dt} = \frac{H^4 - \theta}{H/\hat{a}}$  (23)

289

290 The physical meaning of all variables and governing parameters are the same as in equations (8) – (9), but  
 291 the numerical values and dimensions of some parameters and variables are, indeed, different. Specifically,  
 292  $t(s)$ ,  $H(m)$ ,  $\theta(m^4)$ ,  $\hat{a}(m\ s^{-1})$ ,  $\kappa(m^{-3}s^{-1})$ ,  $c(m^{-3}s^{-1})$ . The casual graph of the dynamical system (22) – (23) is  
 293 shown in Fig. 1 (c).

294 The period of system variability is a function of three governing parameters:

295

296  $P = \varphi(\hat{a}, \kappa, c)$  (24)

297

298 If we choose  $\hat{a}, \kappa$  as parameters with independent dimensions, then according to  $\pi$ -theorem:

299

300  $\frac{P}{\tau} = \Phi\left(\frac{\kappa}{c}\right)$  (25)

301

302  $\tau = (\hat{a}^3 \kappa)^{-1/4}$

303

304 Parameters  $\hat{a}, \kappa, c$  lack in VDP and LP22 models, and therefore we transition to the  $V$ -number that must  
 305 be a function of the same  $\hat{a}, \kappa, c$  parameters:

306

307  $V = \lambda(\hat{a}, \kappa, c)$  (26)

308

309 Since the  $V$ -number is adimensional, and  $\hat{a}, \kappa$  are parameters with independent dimensions, then  
 310 according to  $\pi$ -theorem:

311

312  $V = \Lambda(\kappa/c)$  (27)

313

314 It also means that

315

316  $\frac{\kappa}{c} = \Lambda^{-1}(V)$  (28)

317

318 and we can finally present the VCV18-1  $P$ -scaling law as:

319

320  $\frac{P}{\tau} = \Phi(V)$  (29)

321

322 In other words, the  $P$ -scaling law of the VCV18-1 system is fully defined by the balance between positive  
 323 and negative feedbacks. For  $\tau = 50$  kyr,  $V = 0.63$ ,  $\Phi = 2$ . The corresponding 100-kyr-period auto-  
 324 oscillations of the system (22) – (23) and its positive-versus-negative feedback loop are shown in Fig. 2  
 325 (e, f).

## 326 2.4 VDP model

327 We now consider the VDP model, which is a variant of the historical van der Pol model (1922) used  
 328 by De Saedeleer et al. (2013) and Crucifix (2013) to study synchronization properties of ice ages.

329  $\frac{dx}{dt} = \frac{-\beta - y}{\tau}$  (30)

330 
$$\frac{dy}{dt} = \frac{\alpha}{\tau} \left( y - \frac{y^3}{3} + x \right) \quad (31)$$

331 Here all variables and parameters, except time and timescale  $\tau$ , are adimensional. Variable  $x$  is a proxy for  
 332 the glaciation, and variable  $y$  represents the rest of the climate. Since  $\frac{\tau}{\alpha} \ll \tau$ , for longer, glaciation-like  
 333 processes, we can re-write equations (30) – (31) as:

334 
$$\frac{dx}{dt} = \frac{1}{\tau} \left( -\beta + x - \frac{y^3}{3} \right) \quad (32)$$

335 
$$y - \frac{y^3}{3} + x = 0 \quad (33)$$

336 The equation (33) defines the “critical manifold” (Guckenheimer et al, 2003). The system (32) – (33)  
 337 describes VDP “slow” dynamics between two glacial-interglacial bifurcation points. To get VDP time  
 338 series, we solve the non-idealized system (30) – (31), and we use the system (32) – (33) to visualize  
 339 system’s positive,  $x$ , and negative,  $\frac{y^3}{3}$  feedbacks. Schematically, the dynamical system (30) – (31) is  
 340 shown in Fig. 1 (d). The period of system (30) – (31) variability is the function of two governing  
 341 parameters:

342  
 343 
$$P = \psi(\tau, \beta) \quad (34)$$

344 Only parameter  $\tau$  is dimensional, and therefore according to  $\pi$ -theorem:

345 
$$\frac{P}{\tau} = \Psi(\beta) \quad (35)$$

346 The amplitudes of VDP variables are defined by the critical manifold (33) that does not contain  
 347 parameters  $\tau, \beta$  and therefore both  $x$ - and  $y$ -amplitudes do not depend on model parameters. Consequently  
 348 the amplitudes of positive and negative feedbacks do not depend on them either. In fact, the  $x$ -amplitude  
 349 in VDP model is always  $\sim 0.8$  and  $y$ -amplitude is always 2. Therefore the ratio of the amplitude of the  
 350 positive feedback,  $x$ , to the amplitude of the negative feedback,  $\frac{y^3}{3}$ , is always  $V = 0.3$ . In summary:

351  
 352 
$$V = const \quad (36)$$

353  
 354 The property (36) makes VDP model to be fundamentally different from all other models in this  
 355 study. In all other models, the  $V$ -number is the function of model’s governing parameters and, under  
 356 different scenarios, it changes when parameters change. In the VDP model, the  $V$ -number is pre-defined  
 357 by the model’s structure. Consequently, the scaling law (35) does not contain any  $V$ -number and thus it  
 358 cannot match the scaling law (29). Therefore, *there is no physical similarity* between the VCV18-1 and  
 359 the VDP models.

360 The auto-oscillations of the system (30) – (31) and positive-versus-negative feedback evolution are  
 361 shown in Fig. 2 (g, h). For  $\tau = 50$  kyr and  $\beta = 0.3$ ,  $\Psi = 2.2$ . Fig. 2 (e) and Fig. 2 (g) show well why the  
 362 phenomenological approach may be misleading. For the same internal timescale of 50 kyr, VCV18-1 and  
 363 VDP models both produce asymmetrical (slow growth and fast retreat) glaciation time series with the  
 364 respective periods  $P$  close to 100 kyr, but this occurs because of very different physics: in the VDP model  
 365 the positive feedbacks are much weaker (as we already know,  $V = 0.3$ , always) than in the VCV18-1  
 366 model ( $V = 0.63$ ). Most importantly, this discrepancy cannot be changed, because the VDP model is  
 367 rigid in this regard.

368  
 369  
 370

371 **2.5 LP22 model**

372

373 The LP22 model is described by two differential equations, first, for the growing ice volume,

374 
$$\frac{dv}{dt} = -\frac{I}{\tau_i} + \frac{1}{\tau_g} \quad (37)$$

375 and another one for the diminishing ice volume

376 
$$\frac{dv}{dt} = -\frac{I}{\tau_i} - \frac{v}{\tau_d} \quad (38)$$

377 Here,  $v$  and  $I$  are normalized ice volume and astronomical forcing, correspondingly;  $\tau_i$ ,  $\tau_g$ , and  $\tau_d$  are  
 378 dimensional timescales. Additionally, if  $I < I_0$  the system switches from equation (38) to equation (37),  
 379 and if  $I + v > V_0$ , the system switches from equation (37) to equation (38). Though the original LP22  
 380 model does not consider its evolution without astronomical forcing, oscillations still occur when  $I = 0$  and  
 381 the equation-switching conditions are, correspondingly,  $v \leq V_1$  ( $V_1$  is the minimal, interglacial, volume)  
 382 and  $v \geq V_0$ . Schematically, the dynamical system (37) – (38) with  $I = 0$  is shown in Fig. 1 (e). The period  
 383 of auto-oscillations is a function of four parameters:

384

385 
$$P = \psi(V_0, \tau_g, V_1, \tau_d) \quad (39)$$

386 The parameter  $V_1 \ll V_0$  can be settled as a constant, therefore:

387 
$$P = \psi(V_0, \tau_g, \tau_d) \quad (40)$$

388 If we select  $\tau_g$  as an independent-dimension parameter, then according to  $\pi$ -theorem:

389 
$$\frac{P}{\tau_g} = \Psi(V_0, \tau_d/\tau_g) \quad (41)$$

390 The equation (37) describes a linear ice volume growth implying zero net feedback. This doesn't indicate  
 391 the absence of feedbacks. Indeed, if we are ready to accept that LP22 model is more than just a successful  
 392 fit to empirical data, then for the growing ice sheet, the equation (37) should be consistent with the  
 393 dimensional total mass balance

394

395 
$$\frac{dv}{dt} = \hat{a}S \quad (42)$$

396

397 i.e., changes of ice volume are equal to mass influx  $\hat{a}$  accumulated over its area  $S$ . If we multiply and  
 398 divide  $\hat{a}S$  by ice thickness  $H$ , the total mass balance (42) becomes

399

400 
$$\frac{dv}{dt} = \frac{v}{\tau_g} \quad (43)$$

401

402 where  $\tau_g = H/\hat{a}$ . The equation (43) tells us that the positive feedback  $\frac{v}{\tau_g}$  must be present in the growing  
 403 ice sheet: it relates to the area growth with volume. Its absence in equation (37), therefore suggests that  $\hat{a}$   
 404 has another component that completely compensates for  $\frac{v}{\tau_g}$ , and yet another component that is inversely  
 405 proportional to  $S$  (e.g., continentality effect). Hence, the system (37) – (38) must be written as follows to  
 406 have physical meaning:

407

408  $\frac{dv}{dt} = \frac{1}{\tau_g} + \frac{v}{\tau_g} - \frac{v}{\tau_d}$  (44)

409  $\frac{dv}{dt} = -\frac{v}{\tau_d}$  (45)

410 Schematically, the dynamical system (44) – (45) is shown in Fig. 1 (f). The amplitude of the positive  
 411 feedback is  $\frac{V_0}{\tau_g}$  and the amplitude of the negative feedback is  $\max\left\{\frac{V_0}{\tau_g}; \frac{V_0}{\tau_d}\right\}$ . Since  $\tau_g > \tau_d$ , the  $V$ -number  
 412 therefore is equal to:

413  
 414  $V = \frac{\tau_d}{\tau_g}$  (46)

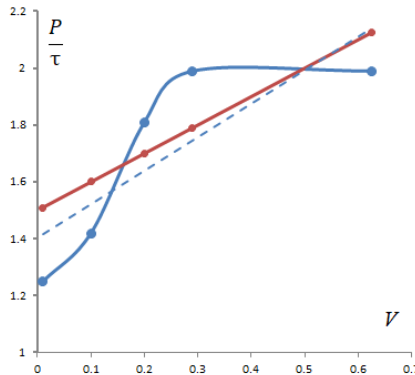
415 Accordingly, the  $P$ -scaling law (41) for LP22 model can be written as

416  $\frac{P}{\tau_g} = \Psi(V_0, V)$  (47)

417 For example, for  $\tau_g = 50$  kyr,  $V_0 = 1.5$ ,  $V_1 = 0.2$ ,  $\tau_d = 20$  kyr, we get  $V = 0.4$  and  $\Psi = 2$ . As we  
 418 have established before, for VCV18-1 model, for  $\tau = 50$  kyr,  $V = 0.63$ ,  $\Phi = 2$ . Therefore, we can talk  
 419 about *physical similarity* between VCV18-1 and LP22 models in terms of reasonably close  $V$ -numbers.

420 The similarity between VCV18-1 and LP22 models becomes very visual in Fig. 2(f) describing the  
 421 positive-versus-negative feedback loops. It can be observed that in VCV18-1 model, during much of ice  
 422 growth, positive and negative feedbacks also completely compensate each other. In fact, we can consider  
 423 LP22 model as being an approximation of the VCV18-1 feedback loop by a triangle. Indeed, the LP22  
 424 positive and negative feedbacks compensate each other during ice advance and when the critical value of  
 425  $v$  (i.e.,  $V_0$ ) is achieved, the system instantly migrates to the single dominant negative feedback. Simply  
 426 speaking, these two models are as similar as the shape of the LP22 feedback-loop triangle in Fig. 2(f) is  
 427 similar to the shape of the VCV18-1 feedback loop, since the  $V$ -number is the ratio of its horizontal  
 428 dimension to its vertical dimension. **This similarity can be illustrated even further if we compare explicit**  
 429 **scaling laws (29) and (47). For this purpose, we solved equations (22) – (23) changing parameter  $c$  and**  
 430 **thus gradually changing the balance between positive and negative feedbacks. The results of these**  
 431 **additional experiments are presented in Fig. 3 together with the  $P$ -scaling law (47) that can be estimated**  
 432 **in a very straightforward manner:  $P \sim V_0 \tau_g + \tau_d$ , or  $\frac{P}{\tau_g} \sim V_0 + \tau_d/\tau_g$ , that is finally  $\frac{P}{\tau_g} \sim V_0 + V$ . It can be**  
 433 **observed that the LP22 scaling law resembles well the VCV18-1 scaling-law trendline thus supporting**  
 434 **our assertion that we can consider LP22 model as an approximation of the VCV18-1 model.**

435

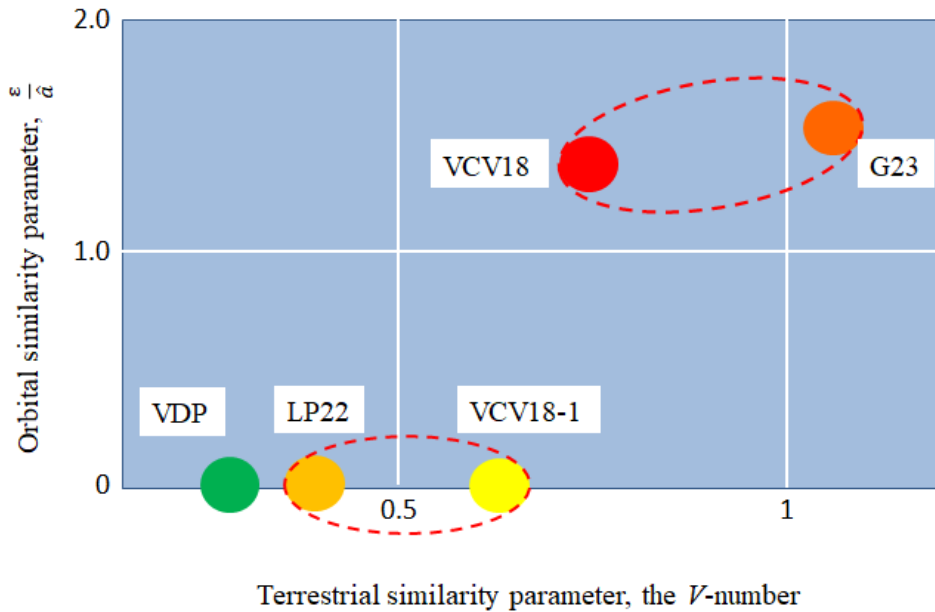


436  
 437 **Fig. 3.** The  $P$ -scaling laws of VCV18-1 (blue, the dotted line is its trendline) and of LP22 (brown)  
 438 models.

439 **3. Conclusions**

440  
 441 Nikolai Gogol would have said: “A magic apple tree may grow golden apples...but not pears”.  
 442 Phenomenological models may not be bounded by a specific physics but they have to be consistent with  
 443 the laws of physics. The concept of physical similarity is what allows us to be vigilant about such  
 444 consistency. Accordingly, we started our presentation with the question: Are phenomenological  
 445 dynamical paleoclimate models physically similar to Nature? We demonstrated that, though they may be  
 446 remarkably accurate in reproducing empirical time series, this is not sufficient to claim physical similarity  
 447 with Nature until similarity parameters are considered. We illustrated such a process of diagnostics of  
 448 physical similarity by comparing three phenomenological dynamical paleoclimate models with the more  
 449 explicit model that played the role of parent dynamical system. Though the nomination of the VCV18  
 450 model to serve as a proxy of the parent dynamical system can, indeed, be questioned, and the  
 451 developments of better proxies should be encouraged, we nevertheless believe that the diagnostics of  
 452 physical similarity, we have described, should become a standard procedure before a phenomenological  
 453 model can be utilized for interpretations of historical records or for future predictions. In other words,  
 454 claiming a model to be a phenomenological one is not an indulgence but a liability.

455 The results of the analysis are summarized in Fig. 4. Here, the physical similarity is visualized as  
 456 proximity between the models in the  $(\frac{\varepsilon}{\bar{a}}, V)$  space.



457  
 458 **Figure 4.** Physical similarity diagnostics for the obliquity-period doubling of the VCV18 and G23 models  
 459 and for 100-kyr auto-oscillations of the VDP, LP22, and VCV18-1 models. The physical similarity is  
 460 visualized here as proximity between the models in the  $\frac{\varepsilon}{\bar{a}} - V$  space. Red dashed ovals embrace models  
 461 which we found to be physically similar and therefore they are in a reasonably close proximity in the  
 462 diagram.

463  
 464 LP22 and G23 models can be considered to be physically similar to particular versions of the VCV18  
 465 model, which amounts to saying that they may be derived from basic laws of physics under some  
 466 reasonable physical assumptions. These findings boost the physical viability of these phenomenological  
 467 models, but this is not unconditional and there are clear boundaries of these phenomenological models  
 468 physical legitimacy. For LP22, the ratio of feedback’s amplitudes, the V-number, is also the ratio of

469 timescales. For the Late Pleistocene and for the Early Pleistocene, all timescales are likely to be different  
470 and physical similarity therefore would need to be re-examined for each period separately. For G23  
471 model, physical similarity was found only for the obliquity-range forcing.

472 Generally speaking, our observation that the VDP model is not physically similar to the simplified  
473 version of the VCV18 model is not a final verdict. It is indeed an indication that VDP is not based on *ice*  
474 physics, but there may be other physical phenomena that may provide physical legitimacy to VDP model.  
475 We are a bit skeptical though that such phenomenon can easily be found, because it would need to be  
476 constrained in the same way as VDP is. Specifically, its ratio of positive and negative feedbacks must to  
477 be fixed to a specific value that never changes.

478 Fig. 4 clearly shows that VDP, LP22 and even VCV18-1 models are not physically similar to the  
479 VCV18 model. Indeed, VDP, LP22, and VCV18-1 scaling laws do not have a similarity parameter that is  
480 a ratio of orbital and terrestrial forcing amplitudes and therefore these models are located on the  
481 horizontal axis of Fig. 4 diagram. Interestingly, VDP, LP22, and VCV18-1 models are located to the left  
482 from the VCV18 and G23 models thus revealing more prominent role of their negative feedbacks. As it  
483 is clearly displayed in the positive-versus-negative feedback diagrams of Fig. 2, it happens because the  
484 mechanism of ice disintegration in these two groups of models is based on very different physics. In  
485 VCV18-1, VDP, and LP22 models, the disintegration of ice sheets happens when the negative feedback  
486 suddenly becomes dominant and destroys an ice sheet. In both VCV18 and G23 models, the  
487 disintegration is due to the additional, fast, positive feedback, which is small during most of the ice-  
488 growth period, but eventually becomes strong enough to boost the orbital forcing that attempts ice  
489 destruction.

490 Importantly, we arrived to the above conclusions without making any effort to somehow artificially  
491 minimize (or maximize) a “distance” between the models in Fig. 4 (though it may be an interesting  
492 separate exercise) but used instead, for the most part, published reference values of model parameters.

493 Also, it should not be forgotten that Fig. 4 is just our attempt to present most important results  
494 visually in one diagram. Since it is 2-dimensional, it demonstrates similarity (or its absence) in terms of  
495 two similarity parameters, the ratio of astronomical forcing amplitude to the terrestrial growth rate and the  
496 positive-to-negative feedback ratio. These two dimensions wouldn't be sufficient if more similarity  
497 parameters need to be visually presented. For example, equation (21) shows that G23 model depends on  
498 the similarity parameter that is the ratio of the orbital period  $T$  to the internal timescale  $1/a$ . This similarity  
499 parameter is absent in the VCV18 model. This absence of similarity, indeed, is not apparent from Fig. 4,  
500 but it is discussed in paragraph 2.2.

501 As a final conclusion, we agree with Saltzman's (2002) proposal that “the essential slow physics is to  
502 be sought in the low-order models.” We observe though that “essential slow physics” that can be derived  
503 from phenomenological models is limited to orbital and terrestrial timescales, to ratios of amplitudes of  
504 orbital and terrestrial forcings, and to ratios of amplitudes of positive and negative feedbacks. This is as  
505 much as phenomenological models can offer, and therefore, we deviate from Saltzman's (2002) further  
506 idea that more explicit models should be tuned to satisfy a best phenomenological model. Instead, we  
507 propose to use available physical models for diagnostics of physical-similarity hypothesis that needs to be  
508 either confirmed or rejected. **Specifically, physical models have to be explored to identify additional  
509 dimensionless quantities playing key roles in their dynamics. Further, finding values for these quantities  
510 should be a central objective of future research into glacial-interglacial dynamics.**

511 Of course, encoding empirical data in a simple mathematical statement will always remain a tempting  
512 possibility. As Grigory Barenblatt (2003) said “Applied mathematics is the *art* of constructing  
513 mathematical models of phenomena in nature...” This means that there are no strict rules on how a piece  
514 of mathematical “art” needs to be produced. Therefore, we do not attempt here to discourage our fellow  
515 “artists” from alluding to phenomenological models. Our goal instead was to remind them about  
516 phenomenological models' limitations and to suggest how these limitations may be addressed.

517

518 **Author contributions:** MYV conceived the research (Verbitsky, 2022b), developed the formalism, and  
519 wrote the first draft of the manuscript. The authors jointly discussed the findings and contributed equally  
520 to the editing of the manuscript.

521 **Competing interests:** The authors declare that they have no conflict of interest.

522 **Acknowledgement:** We are grateful to Andrey Ganopolski for discussions and generous insight into G23  
523 model that includes time series of Fig. 2(c, d), and to Dmitry Volobuev for his help in digitizing VCV18.

524 **We are also grateful to our two anonymous reviewers for their helpful suggestions.**

## 525 **References**

526 Barenblatt, G. I.: *Scaling*, Cambridge University Press, Cambridge, ISBN 0 521 53394 5, 2003.

527 Berger, A. and Loutre, M. F.: Insolation values for the climate of the last 10 million years, *Quaternary*  
528 *Sci. Rev.*, 10, 297–317, 1991.

529 Buckingham, E.: On physically similar systems; illustrations of the use of dimensional equations, *Phys.*  
530 *Rev.*, 4, 345–376, 1914.

531 Crucifix, M.: Why could ice ages be unpredictable?, *Clim. Past*, 9, 2253–2267,  
532 <https://doi.org/10.5194/cp-9-2253-2013>, 2013.

533 De Saedeleer B., Crucifix, M. and Wiczorek, S.: Is the astronomical forcing a reliable and unique  
534 pacemaker for climate? A conceptual model study, *Climate Dynamics*, (40) 273-294 doi:10.1007/s00382-  
535 012-1316-1, 2013.

536 **Ganopolski, A.: *Toward Generalized Milankovitch Theory (GMT)*, *Clim. Past Discuss.* [preprint],**  
537 **<https://doi.org/10.5194/cp-2023-57>, in review, 2023.**

538 Guckenheimer, J., Hoffman, K., and Weckesser, W.: The Forced van der Pol Equation I: The Slow Flow  
539 and Its Bifurcations, *SIAM Journal on Applied Dynamical Systems*, 2, 1-35,  
540 doi:10.1137/S1111111102404738, 2003.

541 Haken, H.: *Information and self-organization: A macroscopic approach to complex systems*. Springer  
542 Science & Business Media, 2006.

543 Kaufmann, R. K., and Pretis, F.: Understanding glacial cycles: A multivariate disequilibrium approach.,  
544 *Quaternary Science Reviews* 251, 106694, 2021

545 Leloup, G. and Paillard, D.: Influence of the choice of insolation forcing on the results of a conceptual  
546 glacial cycle model, *Clim. Past*, 18, 547–558, <https://doi.org/10.5194/cp-18-547-2022>, 2022.

547 Paillard, D.: The timing of Pleistocene glaciations from a simple multiple-state climate model, *Nature*  
548 391, 6665, 378-381, 1998.

549 Saltzman, B.: *Dynamical paleoclimatology: generalized theory of global climate change*, in: Vol. 80,  
550 Academic Press, San Diego, CA, ISBN 0 12 617331 1, 2002.

551 Saltzman, B. and Maasch, K. A.: A first-order global model of late Cenozoic climatic change II. Further  
552 analysis based on a simplification of CO<sub>2</sub> dynamics, *Clim. Dynam.*, 5, 201–210, 1991.



- 553 Saltzman, B. and Verbitsky, M. Y.: Asthenospheric ice-load effects in a global dynamical-system model  
554 of the Pleistocene climate, *Climate Dynamics*, 8, 1-11, 1992.
- 555 Saltzman, B. and Verbitsky, M. Y.: Multiple instabilities and modes of glacial rhythmicity in the Plio-  
556 Pleistocene: a general theory of late Cenozoic climatic change, *Climate Dynamics*, 9, 1–15, 1993.
- 557 Saltzman, B. and Verbitsky, M.: Late Pleistocene climatic trajectory in the phase space of global ice,  
558 ocean state, and CO<sub>2</sub>: Observations and theory, *Paleoceanography* 9, 6, 767-779, 1994
- 559 Talento, S. and Ganopolski, A.: Reduced-complexity model for the impact of anthropogenic CO<sub>2</sub>  
560 emissions on future glacial cycles, *Earth Syst. Dynam.*, 12, 1275–1293, [https://doi.org/10.5194/esd-12-](https://doi.org/10.5194/esd-12-1275-2021)  
561 1275-2021, 2021.
- 562 Tzedakis, P.C., Crucifix, M., Mitsui, T. and Wolff, E.W.: A simple rule to determine which insolation  
563 cycles lead to interglacials. *Nature*, 542(7642), 427-432, 2017
- 564 Tziperman, E., Raymo, M. E., Huybers, P., and Wunsch, C.: Consequences of pacing the Pleistocene  
565 100 kyr ice ages by nonlinear phase locking to Milankovitch forcing, *Paleoceanography*, 21, PA4206,  
566 <https://doi.org/10.1029/2005PA001241>, 2006.
- 567 van der Pol, B.: On oscillation hysteresis in a triode generator with two degrees of freedom, *Philosophical*  
568 *Magazine Series* 6, 43, 700—719, doi:10.1080/14786442208633932, 1922.
- 569 Verbitsky, M. Y.: Inarticulate past: similarity properties of the ice–climate system and their implications  
570 for paleo-record attribution, *Earth Syst. Dynam.*, 13, 879–884, <https://doi.org/10.5194/esd-13-879-2022>,  
571 2022a.
- 572 Verbitsky, M.: Do phenomenological dynamical paleoclimate models have physical similarity with  
573 nature?, *EGU sphere* [preprint], <https://doi.org/10.5194/egusphere-2022-758>, 2022b
- 574 Verbitsky, M. Y. and Chalikov, D. V.: *Modelling of the Glaciers-Ocean-Atmosphere System*,  
575 *Gidrometeoizdat, Leningrad*, edited by: Monin, A. S., 135 pp., 1986.
- 576 Verbitsky, M. Y. and Crucifix, M.:  $\pi$ -theorem generalization of the ice-age theory, *Earth Syst. Dynam.*,  
577 11, 281–289, <https://doi.org/10.5194/esd-11-281-2020>, 2020.
- 578 Verbitsky, M. Y. and Crucifix, M.: ESD Ideas: The Peclet number is a cornerstone of the orbital and  
579 millennial Pleistocene variability, *Earth Syst. Dynam.*, 12, 63–67, [https://doi.org/10.5194/esd-12-63-](https://doi.org/10.5194/esd-12-63-2021)  
580 2021, 2021.
- 581 Verbitsky, M. Y., Crucifix, M., and Volobuev, D. M.: A theory of Pleistocene glacial rhythmicity, *Earth*  
582 *Syst. Dynam.*, 9, 1025–1043, <https://doi.org/10.5194/esd-9-1025-2018>, 2018.